Systems/Circuits

Enhanced $GABA_A$-Mediated Tonic Inhibition in Auditory Thalamus of Rats with Behavioral Evidence of Tinnitus

Evgeny A. Sametsky, Jeremy G. Turner, Deb Larsen, Lynne Ling, and Donald M. Caspary
Department of Pharmacology, School of Medicine, Southern Illinois University, Springfield, Illinois 62794

Accumulating evidence suggests a role for inhibitory neurotransmitter dysfunction in the pathology of tinnitus. Opposing hypotheses proposed either a pathologic decrease or increase of GABAergic inhibition in medial geniculate body (MGB). In thalamus, GABA mediates fast synaptic inhibition via synaptic $GABA_A$ receptors ($GABA_A$Rs) and persistent tonic inhibition via high-affinity extrasynaptic $GABA_A$Rs. Given that extrasynaptic $GABA_A$Rs control the firing mode of thalamocortical neurons, we examined tonic $GABA_A$R currents in MGB neurons *in vitro*, using the following three groups of adult rats: unexposed control (Ctrl); sound exposed with behavioral evidence of tinnitus (Tin); and sound exposed with no behavioral evidence of tinnitus (Non-T). Tonic $GABA_A$R currents were evoked using the selective agonist gaboxadol. Months after a tinnitus-inducing sound exposure, gaboxadol-evoked tonic $GABA_A$R currents showed significant tinnitus-related increases contralateral to the sound exposure. *In situ* hybridization studies found increased mRNA levels for $GABA_A$R δ-subunits contralateral to the sound exposure. Tin rats showed significant increases in the number of spikes per burst evoked using suprathreshold-injected current steps. In summary, we found little evidence of tinnitus-related decreases in GABAergic neurotransmission. Tinnitus and chronic pain may reflect thalamocortical dysrhythmia, which results from abnormal theta-range resonant interactions between thalamus and cortex, due to neuronal hyperpolarization and the initiation of low-threshold calcium spike bursts (Walton and Llinás, 2010). In agreement with this hypothesis, we found tinnitus-related increases in tonic extrasynaptic $GABA_A$R currents, in action potentials/evoked bursts, and in $GABA_A$R δ-subunit gene expression. These tinnitus-related changes in GABAergic function may be markers for tinnitus pathology in the MGB.

Key words: **auditory; GABA; $GABA_A$R; thalamus; tinnitus**

Introduction

Inhibitory neurotransmission is essential for accurate processing of acoustic information. It modulates input/output functions, alters frequency tuning, and sharpens temporal response accuracy while gating neurotransmission to primary auditory cortex (AI; Wang et al., 2008; Edeline, 2011; Richardson et al., 2012). Downregulation of inhibitory function has been suggested to underpin tinnitus pathology in dorsal cochlear nucleus (DCN; Wang et al., 2009; Pilati et al., 2012a; Pilati et al., 2012b), inferior colliculus (IC; Bauer et al., 2008; Dong et al., 2009), and AI (Noreña and Eggermont, 2003; Yang et al., 2007, 2011; Roberts et al., 2012) where tinnitus is accompanied by increased spontaneous activity, bursting, enhanced sound-evoked responses, and reduction in markers of inhibitory neurotransmission (Eggermont and Roberts, 2004; Middleton et al., 2011). This downregulation of inhibitory function is thought to reflect altered homeostatic plasticity compensating for the loss of peripheral excitatory drive (Noreña, 2011; Richardson et al., 2012).

Few studies have examined tinnitus pathophysiology in auditory thalamus/medial geniculate body (MGB). MGB gates the percept of sound as it projects to AI (Banks and Smith, 2011) and limbic structures, which are thought to be involved in individuals most disturbed by their tinnitus (Rauschecker et al., 2010; Leaver et al., 2011). While MGB was historically considered a simple relay of auditory signals between IC and AI, recent studies suggest additional signal processing in MGB (Bartlett and Smith, 1999; Winer et al., 2005; Edeline, 2011; Bartlett, 2013). MGB has intricate reciprocal connectivity with the GABAergic thalamic reticular nucleus (TRN) that regulates attention and sleep (Jones, 1975; Rouiller et al., 1985). The unique connectivity and function of MGB strongly implicates it as a key link in the tinnitus network (Rouiller et al., 1985; Rauschecker et al., 2010; Leaver et al., 2011).

Data from sodium salicylate models of tinnitus suggest altered excitation and inhibition in rat MGB (Su et al., 2012). Proper functioning of MGB is dependent on normal GABAergic inhibition, which in sensory thalamus may account for ~90% of total inhibitory conductance (Belelli et al., 2005; Cope et al., 2005, 2009). In rodents, MGB receives GABAergic projections from IC (Winer et al., 1996; Peruzzi et al., 1997; Ito and Oliver, 2012) and

Received Dec. 12, 2014; revised March 31, 2015; accepted May 12, 2015.

Author contributions: E.A.S., J.G.T., and D.M.C. designed research; E.A.S., D.L., and L.L. performed research; E.A.S., J.G.T., D.L., L.L., and D.M.C. analyzed data; E.A.S., L.L., and D.M.C. wrote the paper.

This research was supported by Office of Naval Research Grant N00014-12-1-0214 and National Institute on Deafness and Other Communication Disorders Grant DC-000151. We thank Drs. Tom Brozoski, Brandon Cox, and Steve Sandstrom for their careful reading and comments on the manuscript.

J.G.T. is the cofounder of OtoScience Labs, which conducts hearing and tinnitus research, and licenses the gap-based testing technology from Southern Illinois University School of Medicine. The authors declare no other competing financial interests.

Correspondence should be addressed to Donald M. Caspary, Southern Illinois University, School of Medicine, Department of Pharmacology, 801 North Rutledge Street, P.O. Box 19629, Springfield, IL 62702. E-mail: dcaspary@siumed.edu.

DOI:10.1523/JNEUROSCI.5054-14.2015

 0270-6474/15/359369-12$15.00/0

TRN (Montero and Scott, 1983; Rouiller et al., 1985), while GABAergic interneurons comprise <1% of MGB neurons (Winer and Larue, 1996). GABAergic inputs to MGB act via postsynaptic $GABA_A$ receptors ($GABA_A$Rs) that are heterogeneous (Sur et al., 1999; Richardson et al., 2012). MGB synapses express low-affinity, fast-desensitizing $GABA_A$Rs (α_1, β_2, γ_2 subunits) that mediate fast synaptic transmission and enable high temporal precision (Mozrzymas, 2004, 2010; Farrant and Nusser, 2005; Barberis et al., 2011). In addition, MGB expresses high levels of $GABA_A$Rs containing α_4- and δ-subunits that mediate nondesensitizing tonic inhibition (Richardson et al., 2011). The presence of the δ-subunit in $GABA_A$Rs results in extrasynaptic location and high agonist affinity, which favors activation by low ambient levels of GABA in extracellular space, which may arise from synaptic spillover and/or release from glia (Farrant and Nusser, 2005; Brickley and Mody, 2012). These nondesensitizing $GABA_A$Rs can generate long-lasting tonic currents that hyperpolarize and shift thalamocortical neurons from tonic to burst-firing mode. This shift could alter the salience of phantom acoustic signals to AI.

GABAergic inhibition is critically involved in determining higher-frequency thalamocortical oscillations as well as slow-wave sleep (Llinás and Steriade, 2006). Llinás et al. (2005) postulated that excessive inhibition in thalamus could be the origin of pathologically increased hyperpolarization of thalamic neurons, resulting in deinactivation of T-type Ca^{2+} channels. Upon depolarization, these channels generate low-threshold burst spikes in the wakeful state. A proposed thalamocortical dysrhythmia model suggests that elevated inhibition and the resultant focal burst activity associated with abnormal low-frequency oscillations in thalamus produce ectopic disinhibition of fast oscillatory activity in AI that could correlate with tinnitus (Llinás and Steriade, 2006).

Using *in vitro* patch-clamp recordings, we sought to clarify the role of $GABA_A$ inhibition in MGB as it relates to tinnitus pathophysiology in a sound-exposure behavioral model of tinnitus. In contrast to findings from other auditory structures, MGB circuits showed an increase in $GABA_A$R function in animals with behavioral evidence of tinnitus.

Materials and Methods

Young-adult (3–4 months) Long–Evans male rats (Harlan Laboratories) were housed on a 12 h reversed light/dark cycle with *ad libitum* access to food and water. Forty-five Long–Evans rats were used for electrophysiological recordings in the MGB slice preparation and 13 Fischer Brown Norway (FBN) rats from earlier tinnitus experiments (Wang et al., 2009) were used for MGB *in situ* hybridization studies. Both strains have similar life expectancy, with young adult animals used in both studies.

All experiments were conducted in strict accordance with a protocol approved by the Animal Care and Use Committee of Southern Illinois University.

Noise exposure and induction of tinnitus. Tinnitus was induced between 3 and 4 months of age, using methods similar to those described by Bauer et al. (1999) and Bauer and Brozoski (2001). Briefly, acoustic exposure was a 16 kHz octave band at 116 dB SPL into one ear of a ketamine/xylazine anesthetized rat for 1 h. This exposure typically results in an ipsilateral 30–40 dB temporary threshold shift [measured as pre-to-post noise exposure shift in auditory brainstem response (ABR) thresholds] across frequencies, with increased threshold elevations at frequencies near the 16 kHz exposure (Wang et al., 2009). The exposure also produces a small, variable, permanent ipsilateral threshold shift as measured by ABR (Wang et al., 2009). Acoustic nerve fiber losses were not measured in this set of sound-exposed rats (Bauer et al., 2007; Kujawa and Liberman, 2009). Prepulse inhibition (PPI) was assessed in parallel with gap detection performance. ABR and prepulse findings suggest that gap detection was not altered by unilateral hearing loss at the levels used in these studies (Turner et al., 2006).

Behavioral testing. The gap detection reflex method was adapted from Turner et al. (2006) and Turner (2007), and was based upon the ability of the acoustic startle reflex to be reduced when preceded by a silent gap in a constant acoustic background. As detailed in Wang et al. (2009), behavioral testing used Kinder Scientific startle reflex hardware and software, which was customized for this application. Background sounds were presented through one speaker (XT25TG30-04, Vifa) with startle stimuli presented through a second speaker (CTS KSN-1005, PowerLine). A piezoelectric transducer provided the measure of startle force applied to the floor. An animal holder was suspended above the floor, allowing the animal to freely turn around while minimizing excessive movement. The sound-gap envelope consisted of 60 dB peak (SPL) broadband noise (BBN) or filtered noise (one-third octave bandpass, 48 dB/octave roll off, Model 3988, Krohn-Hite) centered at 10, 12.5, 16, 20, and 25 kHz, calibrated at 60 dB peak SPL. PPI was measured in parallel as a hearing level control and to test for hyperacusis (Turner and Parrish, 2008). Animals with threshold elevation and/or showing hyperacusis were eliminated from the study. Two months after noise exposure, animals were behaviorally tested twice on different occasions, and the results of two sessions were averaged to determine tinnitus. Gap/PPI test sessions began with a 1 min acclimation period followed by two trials consisting of the startle-eliciting noise burst (115 dB SPL, 20 ms duration), which served to habituate the startle response to a more stable baseline. Data from these two initial trials were not used in the gap detection analysis. The remainder of the session consisted of startle-only trials mixed with gap or PPI trials (Turner et al., 2006; Kalappa et al., 2014).

The intertrial interval varied throughout test sessions, with targeted frequencies and BBN stimuli for both gap and PPI presented in ascending order from 10 kHz to BBN (380 trials per session). Gap and prepulse stimuli occurred 100 ms before the startle stimulus and were 50 ms long with a 1.0 ms rise/fall time (Turner et al., 2006). Acoustic stimuli were calibrated using a cloth model rat and a Brüel & Kjær Pulse System with a 0.5 inch free-field microphone (model 4191, Brüel & Kjær). Ambient sound levels in test chambers (with background test noise turned off) were <20 dB SPL in the 4–40 kHz range.

Tinnitus determination. Data from gap detection and PPI testing were expressed as the ratio of mean startle response for a gap or PPI trial relative to a proximal startle-only trial (for details, see Kalappa et al., 2014). A response of 1.0 meant that the startle reflex was the same whether or not it was preceded by a gap or prepulse stimulus. The lower the ratio is from 1.0, the greater the startle inhibition. An individual subject's average data from the two behavioral test sessions were inspected for freedom from artifacts, such as a high level of ambulatory movement. Tinnitus index scores were calculated by subtracting the PPI ratio from the gap ratio. Higher scores are indicative of tinnitus-like deficits in processing silent gap cues. This index score provides a metric that describes the response of an animal to silent gap cues relative to control sounds and helps control for several potential confounds in the gap ratio as a standalone metric for tinnitus. The index score helps to control for hearing loss as an inability to hear or process the 60 dB test stimulus, which would result both in poor gap ratios and poor PPI ratios, hence a small score. The index also helps to control for startle reflex amplitude differences. If an animal has such a small startle reflex that it cannot be inhibited by a silent gap cue, the same impact would be found in the PPI testing where small startle reflexes would also be expected, again resulting in a small index score. This metric controls for temporal processing deficits, which should be present in both the gap and PPI conditions, given their identical timing features. Finally, this index corrects for nonspecific sensory gating/filtering failures, which should impact both gap and PPI response ratios. Mean tinnitus index scores for control animals were pooled to obtain the average control group startle ratio, with 95% confidence intervals determined for each frequency and BBN.

The average tinnitus index score for each noise-exposed subject was compared with the average control tinnitus index score for that frequency. Noise-exposed subject responses that fell within the 95% confidence interval for the control group were deemed no different from those

of control subjects and were without tinnitus for that given frequency or BBN. Noise-exposed subjects with tinnitus index scores reduced beyond the 95% confidence interval of the companion control group were considered significantly different. These subjects were considered to have tinnitus at that given frequency or BBN.

In situ *hybridization.* Adult (4 months old) male FBN rats were used for *in situ* hybridization experiments. The animals were repurposed from a prior series of similarly conducted tinnitus experiments with the identical sound exposure conditions. Previously, we published patch-clamp recordings of gaboxadol (GBX)-evoked tonic $GABA_A$R currents from MGB neurons in adult FBN rats (Richardson et al., 2011, 2013). The recorded parameters of gaboxadol-evoked tonic $GABA_A$R currents in FBN rats were comparable to those presented here for Long–Evans rats. Animals were divided into the following two groups: sound exposed and control/sham exposed. These animals were not assigned a tinnitus score. *In situ* hybridization studies were conducted as described by Ling et al. (2005). Oligonucleotide probes for α_4 (Wisden et al., 1991; 5′-CAA GTC GCC AGG CAC AGG ACG TGC AGG AGG GCG AGG CTG ACC CCG-3′) and δ (provided by Merck Inc.; 5′-GAC CTT GGC TTT CCG TTT CTT CCT GTA GTC AGC ATT-3′) were synthesized and purified by Sigma-Genosys. The probes were then 3′-end labeled with ^{35}S-dATP (NEN-PerkinElmer Life Science) by 3′-terminal deoxynucleotidyl transferase using a commercially available kit (Fisher Scientific), and purified and desalted through a micro BioSpin-30 column (Bio-Rad). These labeled probes were used to detect $GABA_A$R subunits α_4 and δ in MGB. Additional methods, visualization, and quantification were performed as in the study by Richardson et al. (2013).

All slides were blinded to ensure unbiased measurement. The accumulation of silver grains over cell bodies (~10 times above slide background) was interpreted as positive hybridization labeling for the α_4 and δ $GABA_A$R subunits to their specific mRNAs. Only grains within the perimeter of the cell were counted. Data were collected from cells only if they were distinguishable as individual cells possessing a nucleolus. The numbers of grains over somata of MGB neurons (silver grains/100 μm^2) were counted, and values were corrected by subtracting background labeling obtained from five random off-tissue areas on each slide.

Preparation of thalamic brain slices for electrophysiology. Two months following sound exposure and within 2 weeks of behavioral testing, Long–Evans rats (5–7 months old) were anesthetized with isoflurane and decapitated. Brains were rapidly removed, and horizontal brain slices (300 μm) were cut using a VT 1000P vibratome (Leica Microsystems) in ice-cold (<4°C) sucrose-rich artificial CSF (aCSF) containing the following (in mM): sucrose 250, KCl 3, NaH_2PO_4 1.23, $MgCl_2$ 5, $CaCl_2$ 0.5, $NaHCO_3$ 26, and glucose 10, pH 7.4, saturated with carbogen (95% O_2/5% CO_2). Slices were retained in a holding chamber filled with standard aCSF containing the following (in mM): NaCl 124, KCl 3, KH_2PO_4 1.25, $MgCl_2$ 1.3, $CaCl_2$ 2, $NaHCO_3$ 26, and glucose 10, pH 7.4, saturated with carbogen and warmed to 32°C for 20 min before being allowed to equilibrate to room temperature (~22°C) for at least 1 h before recording. Slices were transferred to a submersion recording chamber mounted on the stage of an upright Olympus BX-51WI microscope, maintained at room temperature, and continuously perfused with standard aCSF saturated with carbogen, at a flow rate of 2 ml/min using a peristaltic P720 pump (Instech Laboratories).

Electrophysiology. Using infrared differential interference contrast microscopy, visually guided, somatic, whole-cell patch-clamp recordings were obtained from MGB neurons using fire-polished borosilicate glass electrodes (4–5 MΩ). Two intracellular solutions were used in this study. In voltage-clamp experiments, patch electrodes were filled with the following (in mM): 120 CsMeSO3, 2 CsCl, 5 NaCl, 1.5 MgCl2, 10 HEPES, 10 EGTA, 5 TEA-Cl, 2.5 Mg-ATP, 0.3 Na-GTP, and 5 QX-314, pH 7.3, adjusted with CsOH, with osmolarity of 290 ± 10 mOsm. In current-clamp experiments, a more "physiological" solution was used, as follows: K-gluconate140, NaCl 1, $MgCl_2$ 2, Mg-ATP 2, Na-GTP 0.3, and HEPES 10, pH 7.3–7.4, adjusted with KOH, with osmolarity of 290 ± 10 mOsm. Holding potentials were not corrected for the liquid junction potential. Voltage-clamp and current-clamp recordings were obtained using a MultiClamp-700B amplifier and Digidata-1440A analog-to-digital converter (Molecular Devices). The signal was low-pass filtered at 5 kHz and digitized at 10 kHz. Data were acquired using pClamp 10 software (Molecular Devices). For all recordings, series resistance was <20 MΩ and was monitored continuously.

To isolate GABAergic currents, 20 μM 6,7-dinitroquinoxaline-2,3-dione (DNQX) and 50 μM D(−)-2-amino-5-phosphonopentanoic acid (D-AP5) were added to the standard aCSF. Extrasynaptic tonic $GABA_A$R currents were evoked by bath application of the selective agonist, 0.1–10 μM gaboxadol [4,5,6,7-tetrahydroisoxazolo[5,4-c]pyridine-3(2H)-one], in the presence of glutamatergic receptor blockers. $GABA_A$ tonic currents and spontaneous IPSCs (sIPSCs) were recorded at −10 and +20 mV, respectively. $GABA_A$ currents were blocked with 40 μM gabazine.

Drugs. Drugs were dissolved in distilled water to a concentration of 1–10 mM, and the stock solutions were divided into small aliquots and frozen. The following stock drug solutions were used to prepare fresh final solutions every day: QX-314 from Tocris Bioscience; DNQX, D-AP-5, and gabazine from Abcam; with all other chemicals from Sigma-Aldrich.

Analysis. Postrecording analyses of extrasynaptic $GABA_A$R currents and action potential firing evoked using current steps were analyzed using pClamp 10. Dose–response curve fitting was performed in Origin 8 (OriginLab) using an iterative process to minimize the χ^2 test. Spontaneous IPSCs were analyzed using MiniAnalysis version 6.0.3 software (Synaptosoft). All spontaneous IPSPs were visually verified on the basis of event kinetics. Between 500 and 1500 individual events were analyzed for each cell (4 min of gap-free acquisition).

All statistical values were evaluated with Origin 8 (OriginLab) or SAS/STAT (SAS Institute). Values are presented either as the mean ± SEM or mean ± SD (box plot). ANOVA with Tukey's *post hoc* analysis was used when multiple comparisons were made. Pairwise group differences were evaluated using a Student's *t* test. Statistical significance was established at $p \leq 0.05$.

Results

For all voltage-clamp studies examining tonic and synaptic $GABA_A$ currents, analyses were performed on the following three groups: (1) 10 control (Ctrl) rats; (2) 14 sound-exposed rats with behavioral evidence of tinnitus (Tin); and (3) 4 sound-exposed without tinnitus (Non-T). Current-clamp experiments examined membrane properties and burst properties, used eight animals with behavioral evidence of Tin, which compared with nine Ctrls (Fig. 1). Current-clamp studies compared only two groups because of the low availability of exposed non-hearing loss animals reliably identified as Non-T. Figure 1 shows the pooled behavioral data for both experimental groups with significant differences for the broadband noise gap background condition for all groups.

The MGB can be divided into the following three distinctive subdivisions: lemniscal ventral MGB (vMGB), non-lemniscal dorsal MGB (dMGB), and medial MGB (mMGB; Fig. 2). In the present study, patch-clamp recordings were localized to vMGB or dMGB, contralateral to the sound exposure.

Membrane properties of MGB neurons

Immediately following entry into whole-cell mode, the basic membrane parameters, including resting membrane potential (V_{rest}), input resistance (R_m), whole-cell membrane capacitance (C_m), and membrane time constant (τ) were measured. Measurements of V_{rest} were obtained by briefly switching to current-clamp mode. R_m and C_m were measured in voltage-clamp mode at 0 holding current with 5 mV hyperpolarizing pulses that were 50 ms in duration. Although V_{rest}, R_m, C_m, and τ were measured in all neurons, the mean data shown in Table 1 were calculated using the K-gluconate internal solution (see Materials and Methods), as this solution most faithfully replicates physiological conditions. Pairwise differences were evaluated using a two-tailed

Student's t test. No significant tinnitus-related changes were observed in the resting membrane potential of MGB neurons (dMGB: Ctrl, −70.7 ± 1.7 mV, $n = 18$; and Tin, −68.8 ± 1.6 mV, $n = 15$, $p = 0.44$; vMGB: Ctrl, −72.5 ± 2.0 mV, $n = 17$; and Tin, −72.5 ± 2.31 mV, $n = 15$, $p = 0.99$). Membrane input resistance had a slight tendency to be higher in Tin animals, but differences were nonsignificant (dMGB: Ctrl, 377.5 ± 37.4 MΩ, $n = 18$; and Tin, 422.9 ± 39.1 MΩ, $n = 15$, $p = 0.41$; vMGB: Ctrl, 407.9 ± 39.6 MΩ, $n = 17$; and Tin, 420.1 ± 44.7 MΩ, $n = 15$, $p = 0.84$). Similarly, the C_m and τ of MGB neurons were not affected by traumatic sound exposure and tinnitus pathology. Basic passive membrane properties of MGB neurons also did not differ significantly between dorsal and ventral MGB subdivisions (Table 1).

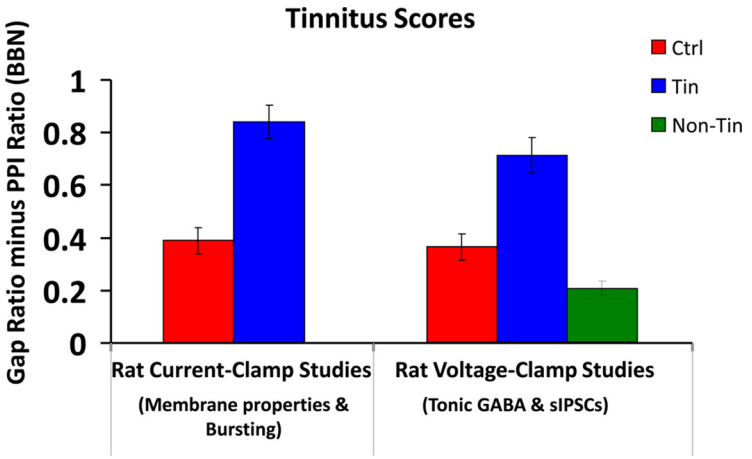

Figure 1. Mean tinnitus scores for BBN in animals. Mean tinnitus scores for Long–Evans rats used in current-clamp experiments [red, Ctrl ($n = 8$); blue, Tin ($n = 9$)] and voltage-clamp experiments [red, Ctrl ($n = 10$); blue, Tin ($n = 14$); green, Non-T ($n = 4$)]. Left panels correspond to a first cohort of animals used for measuring MGB neurons passive membrane and firing properties (current clamp). Right panel represents a second set of animals used for measuring $GABA_A$R currents (voltage clamp). Tinnitus index scores were calculated by subtracting PPI ratios from gap ratios (see Materials and Methods). Higher tinnitus scores suggest a deficit processing silent gap cues relative to other sounds. Error bars indicate ±SEM.

Tinnitus MGB neurons generate increased numbers of spikes per burst

Changes in the action potential firing properties of MGB neurons related to tinnitus were investigated in the experimental set with K-gluconate internal solution. In agreement with previous reports, the majority of neurons in both Ctrl and Tin groups responded with burst-firing mode upon somatic positive current injection. Representative traces of burst-firing neurons from Ctrl and Tin animals are shown in Figure 3. In accord with previous reports, bursting neurons had a more negative resting membrane potential compared with regular spiking neurons. Although there were no significant group differences in the number of burst-firing neurons (Ctrl, 62.9%; Tin, 66.7%; Table 1), Tin rats tended to have more bursting neurons in the vMGB division (Ctrl, 58.8%; Tin, 73.3%; Table 1). Most importantly, Tin rats showed a significant increase in the number of spikes per burst (4.2 ± 0.4, $n = 20$) compared with Ctrl (2.9 ± 0.4, $n = 24$) when evoked using suprathreshold current steps (Fig. 3). Tin versus Ctrl differences in spikes per burst were more evident in the vMGB (vMGB: Ctrl, 2.4 ± 0.5, $n = 11$; and Tin 4.6 ± 0.7, $n = 11$; dMGB: Ctrl, 3.4 ± 0.5, $n = 13$; and Tin 3.7 ± 0.4, $n = 9$). This tinnitus-related increase in the number of spikes per burst was not directly related to higher input resistance or a difference in resting membrane potential (Table 1).

We further examined whether changes in the low-threshold Ca^{2+} conductance might underpin the tinnitus-related increase in the number of spikes per burst. Bursts generated after the offset of hyperpolarizing current injection showed no tinnitus-related differences in amplitude or area of low-threshold Ca^{2+} spikes (LTSs; Fig. 4*A*,*B*). This suggests that tinnitus-related altered excitability may involve additional mechanisms and that further investigation will be required.

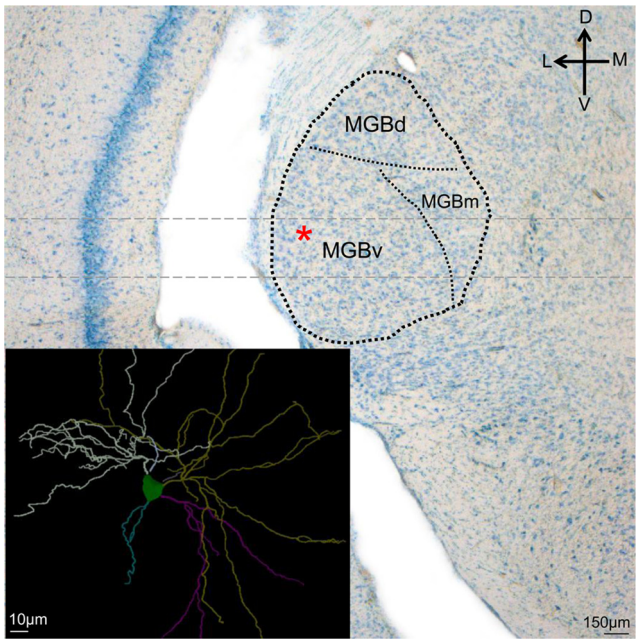

Figure 2. Thionin-stained coronal section through MGB. dMGB, vMGB, and mMGB divisions are demarcated by dotted black lines. The gray dashed line represents the horizontal sectioning plane for making acute brain slices containing MGB. Inset represents a recorded MGB neuron that was labeled with neurobiotin and traced using Neurolucida. The red star mark defines the location of the neuron in MGB.

Gaboxadol-evoked tonic $GABA_A$R currents are elevated in MGB neurons from Tin rats

We evaluated the tinnitus-associated behavior of $GABA_A$R tonic inhibition in MGB neurons via application of the GABA analog GBX, which at low (micromolar) concentrations selectively activates $GABA_A$Rs containing $\alpha_4\delta$-subunits. Similar to previous reports (Richardson et al., 2011, 2013), bath application of 5 μM GBX activated extrasynaptic $GABA_A$Rs on MGB neurons and resulted in a negative ~8 mV hyperpolarizing membrane potential shift that changed MGB neuronal discharge properties from tonic firing to burst mode in response to identical depolarizing current steps (Fig. 5).

Extrasynaptic $GABA_A$R currents were evoked by bath application of increasing concentrations of GBX (0.1–10 μM) in the presence of glutamate receptor blockers (Fig. 4*A*). Voltage-clamp recordings were performed at −10 mV to increase the Cl^- driving force. Each incremental dose was applied for 5 min, with peak amplitude of $GABA_A$R currents measured over a 30 s period. To verify the GABAergic nature of the evoked current, 40 μM gaba-

Table 1. Membrane properties and discharge mode of MGB neurons

		Parameters						
Condition	MGB division	*n*	V_{rest} (mV)	C_m (pF)	R_m (MΩ)	τ (μs)	Depth (μm)	Bursting/ regular spiking (*n*)
Ctrl	Dorsal	18	−70.67 ± 1.73	143.38 ± 8.13	377.48 ± 37.42	2.53 ± 0.14	39.90 ± 2.26	12/6
	Ventral	17	−72.50 ± 1.97	129.50 ± 6.64	407.89 ± 39.58	2.23 ± 0.12	41.39 ± 2.58	10/7
Tin	Dorsal	15	−68.80 ± 1.64	133.27 ± 7.98	422.87 ± 39.10	2.51 ± 0.20	41.00 ± 2.77	9/6
	Ventral	15	−72.53 ± 2.31	125.67 ± 8.60	420.13 ± 44.66	2.33 ± 0.21	43.67 ± 3.70	11/4

Values are given as the mean ± SEM, unless otherwise indicated. Statistical analysis did not reveal significant difference between Ctrl and Tin groups in all parameters presented in the table. Similarly, no difference was found between dMGB and vMGB neurons. Depth, MGB neurons depth from a slice surface (μm).

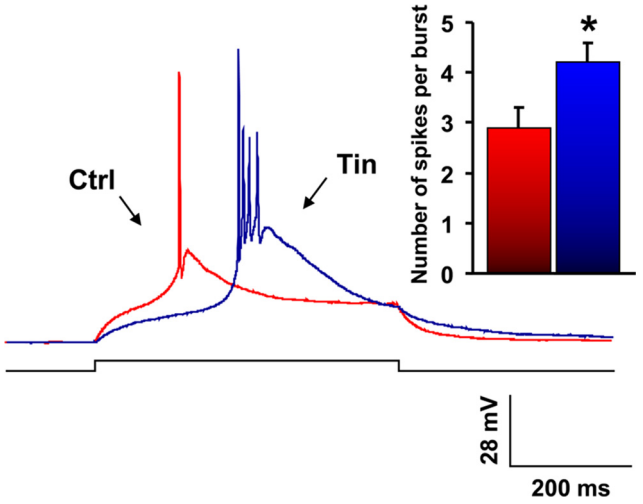

Figure 3. MGB neurons from the Tin group demonstrated increased spiking during bursting. The injection of positive current, 500 ms, activates a low-threshold Ca^{2+} spike that generates burst firing in a majority of MGB neurons. Representative recordings from MGB neurons showing burst firing from a control animal (red; V_{rest}, −76 mV; 80 pA current step) and from a rat with behavioral evidence of tinnitus (blue; V_{rest}, −76 mV; 50 pA current step). The number of spikes per burst was significantly increased in tinnitus animals. Burst per spike latency was not different among groups. Representative traces with different burst/spike latency were selected for clarity of demonstration only. Insert showing the mean number of spikes per burst in the Ctrl and Tin groups of rats. Error bars indicate ±SEM. *$p < 0.05$, *t* test.

zine, a nonselective $GABA_A$R antagonist, was applied at the end of each GBX dose series. The peak amplitude of the $GABA_A$R tonic current was measured with reference to current recorded following gabazine application. Most MGB neurons showed current saturation at the maximum (10 μM) GBX concentration used in these experiments. Higher GBX concentrations were not used to avoid concomitant activation of synaptic $GABA_A$Rs.

We recorded from 32 MGB neurons from 10 Ctrl rats, 43 neurons from 14 Tin rats, and 11 neurons from 4 Non-T rats. All recordings were contralateral to the sound exposure and were parsed by subdivision into recordings from dMGB and vMGB (dMGB/vMGB, respectively: Ctrl, 16/16 neurons; Tin, 20/23 neurons; Non-T, 5/6 neurons).

Repeated-measures ANOVA revealed significant differences among three experimental groups in the dose–response amplitude of $GABA_A$R tonic currents, measured with bath application of 0.1–10 μM GBX ($F = 3.15$; $p = 0.048$; Fig. 6). There was significant interaction between GBX concentrations and groups ($p = 0.037$). Additional *t* test analysis demonstrated significant increases in the amplitude of $GABA_A$R tonic currents for the Tin group compared with the Ctrl group at 1–10 μM GBX concentrations (1 μM GBX, $p = 0.034$; 2 μM GBX, $p = 0.022$; 5 μM GBX, $p = 0.012$; 10 μM GBX, $p = 0.019$; Fig. 6). No differences were found between the Non-T group and either the Ctrl or Tin groups. Figure 6*D* shows the significant 25.5% increase in mean current amplitude in the Tin group compared with the Ctrl group at 10 μM GBX (Ctrl, 217.11 ± 14.86 pA; Tin, 272.54 ± 16.66 pA; Non-T, 259.08 ± 20.02 pA). Likewise, a 19.1% greater current density occurred in the Tin group ($p = 0.02$) relative to Ctrl (Ctrl, 1.83 ± 0.11 pA/pF; Tin, 2.18 ± 0.08 pA/pF; Non-T, 2.09 ± 0.1 pA/pF; Fig. 6*E*). No significant differences were identified between the Non-T group and either the Ctrl or Tin groups at a 10 μM GBX concentration. $GABA_A$R tonic currents were comparable in dMGB and vMGB across groups [e.g., the 25% tinnitus-related increase in maximal current was detected in dMGB and vMGB at 10 μM GBX, but only reached significance in dMGB ($p = 0.046$) when comparing current density in the smaller parsed groups].

When the dose–response curves were normalized to the maximal current recorded with 10 μM GBX, a simple logistic function was used to fit dose–response data from which the EC_{50} and activation slope for $GABA_A$R tonic current were calculated for each individual neuron. Importantly, no decline in $GABA_A$R function was observed for any of the functional parameters examined. No significant group differences were seen for mean EC_{50} (Ctrl, 2.60 ± 0.36 μM; Tin, 1.95 ± 0.21 μM; Non-T, 2.29 ± 0.49 μM) or activation slope (Ctrl, 1.6 ± 0.06; Tin, 1.61 ± 0.05; Non-T, 1.42 ± 0.06; Fig. 6*C*). Since no group differences were found in current kinetics, it was concluded that tinnitus pathology does not substantially alter the subunit makeup of extrasynaptic $GABA_A$Rs.

This tinnitus-associated augmentation of GBX-evoked currents suggests an increase in the number of extrasynaptic $GABA_A$Rs. The significant increase in tonic currents in Tin animals differs dramatically from the near 50% loss of similarly evoked tonic currents recorded previously from aged MGB neurons (Richardson et al., 2013).

δ-Subunit expression is upregulated contralateral to sound exposure in Tin group

To assess the possibility of $GABA_A$R subunit changes underpinning the tinnitus-related increases in MGB neuronal $GABA_A$R tonic currents, *in situ* hybridization was used to examine the expression of the $GABA_A$R α_4- and δ-subunits, markers of tonic–current extrasynaptic $GABA_A$R constructs. Previous radioligand binding and immunohistochemical studies using [^{3}H]gaboxadol and antibodies for α_4- and δ-subunits suggested exceptionally high levels of the $\alpha_4\delta$-subunit containing extrasynaptic $GABA_A$Rs in MGB (Richardson et al., 2012; Richardson et al., 2013). Similarly, the present *in situ* hybridization study found high expression levels of $\alpha_4\delta$ $GABA_A$R subunits throughout MGB (Fig. 7).

Again, contrary to what was predicted, *t* test hypothesis testing revealed a significant increase in mRNA expression of the $GABA_A$R δ-subunit contralateral to sound exposure both in dMGB and vMGB (dMGB: Ctrl, 2.9 ± 0.34 silver grains/100

μm^2; Tin, 5.6 ± 0.27 grains/100 μm^2; $p <$ 0.001; vMGB: Ctrl, 3.0 ± 0.29 grains/100 μm^2; Tin, 5.5 ± 0.22 grains/100 μm^2; $p <$ 0.001). Replacing the γ-subunit with the δ-subunit results in $GABA_A$Rs with extrasynaptic receptor location and tonic inhibitory currents. Figure 7 summarizes changes in α and δ $GABA_A$R subunit mRNA levels associated with behavioral evidence of tinnitus. These gene expression data support the patch-clamp findings described above, suggesting that tinnitus pathology may result in an increase in extrasynaptic $GABA_A$R density. Interestingly, α-containing $GABA_A$Rs showed significant tinnitus-related mRNA increases in MGB ipsilateral to the sound exposure (dMGB: Ctrl, 6.0 ± 0.2 grains/100 μm^2; Tin, 9.0 ± 0.25 grains/100 μm^2; $p < 0.001$; vMGB: Ctrl, 5.5 ± 0.21 grains/100 μm^2; Tin, 9.7 ± 0.25 grains/100 μm^2; $p < 0.001$) with only modest, nonsignificant increases contralateral to the sound exposure (Fig. 7).

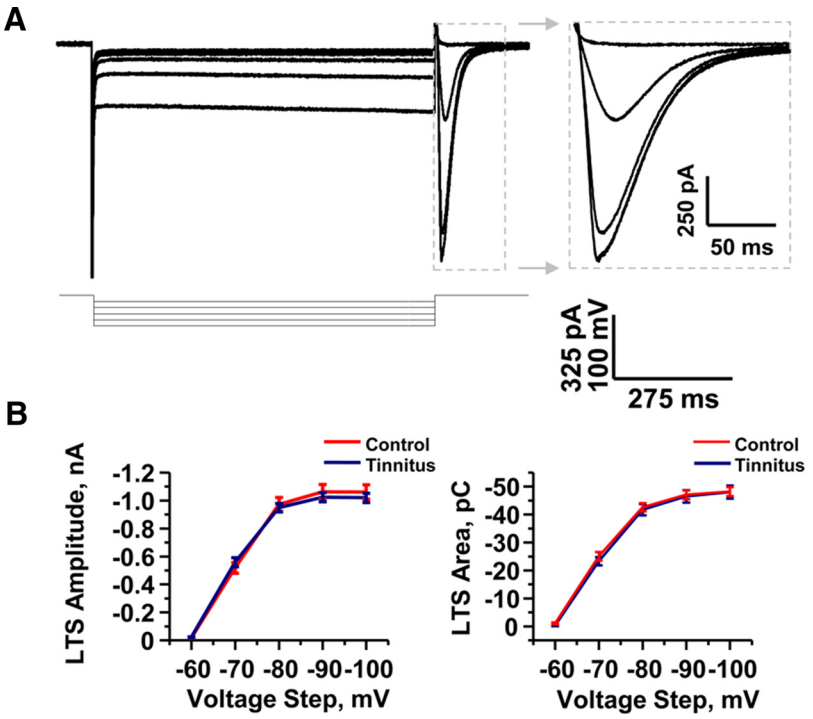

Figure 4. LTSs underlying MGB neuronal bursting showed no tinnitus-related differences in amplitude or area. ***A***, Representative recording from a Ctrl animal. MGB neurons were held at −50 mV to inactivate low-threshold Ca^{2+} channels. Subsequent hyperpolarizing voltage steps, 500 ms, remove channel inactivation and deactivate the channels. LTS current was generated after the offset of the hyperpolarizing voltage step. Inset, Magnified portion of the current traces after the hyperpolarizing voltage steps. ***B***, LTS current amplitude and area [red, Ctrl ($n = 39$ cells); blue, Tin ($n = 30$)] plotted against varying hyperpolarizing steps. Data are presented as the mean ± SEM.

Ambient GABA and resting membrane potential of MGB neurons

Given the presence of high-affinity extrasynaptic $GABA_A$Rs on MGB neurons, it is feasible that these receptors would be tonically active in the presence of low concentrations of ambient GABA in the extracellular space. We evaluated the possible role of endogenous tonic $GABA_A$R currents on resting membrane potential and firing properties of MGB neurons, with bath application of gabazine. MGB neurons from Ctrl and Tin groups were recorded in current-clamp mode with no correcting currents applied to clamped neurons, and blockers of glutamatergic synaptic transmission omitted from the recording solution. Ten minutes after obtaining whole-cell configuration, baseline resting membrane potential was recorded for 5–10 min followed by recording in aCSF solution with gabazine (40 μM) for another 15 min. The membrane potential change (ΔV) calculated by subtracting $V_{gabazine}$ (10 min following gabazine application) from V_{rest} (measured immediately before gabazine application). V_{rest} and $V_{gabazine}$ were mean values calculated over a period of 1 min. Bath application of gabazine to MGB slices blocked synaptically mediated IPSPs, and in some recordings resulted in a small depolarizing shift (3–4 mV) in V_{rest}. However, the depolarizing shift of gabazine on baseline V_{rest} was not significant in both the Ctrl and Tin groups.

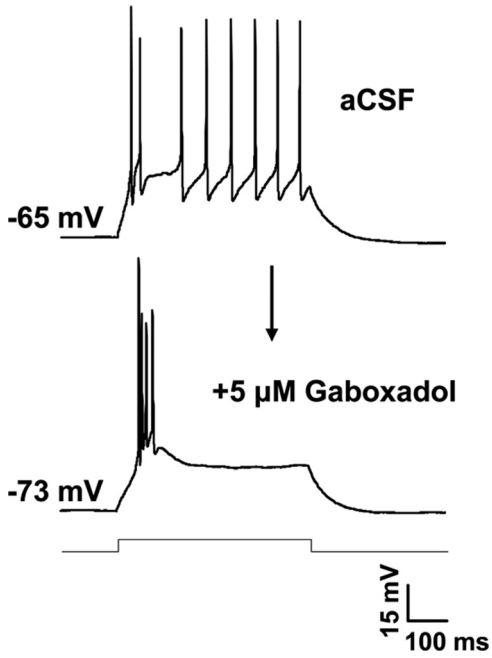

Figure 5. Gaboxadol tonically activates extrasynaptic $GABA_A$Rs, hyperpolarizes resting membrane potential, and converts MGB neurons to burst mode. Top trace shows a representative recording from a tonically firing MGB neuron. Bath application of 5 μM GBX hyperpolarizes (Δ8 mV) the membrane potential, deactivating low-threshold Ca^{2+} channels, and converted this MGB neuron to burst-firing mode.

Synaptic sIPSCs in auditory thalamus are not affected by sound exposure

We further examined whether GABAergic changes at extrasynaptic receptors were associated with changes in synaptic GABA transmission. For this purpose, we compared sIPSCs in MGB neurons in Ctrl and Tin animal groups. sIPSC activity was recorded for 4–5 min from MGB neurons contralateral to sound exposure. Recordings were from the same set of neurons in which extrasynaptic $GABA_A$R currents were tested before GBX dose–response experiments.

Typical recordings of sIPSCs from MGB neurons are demonstrated in Figure 6*A*. Recordings were made at +20 mV to max-

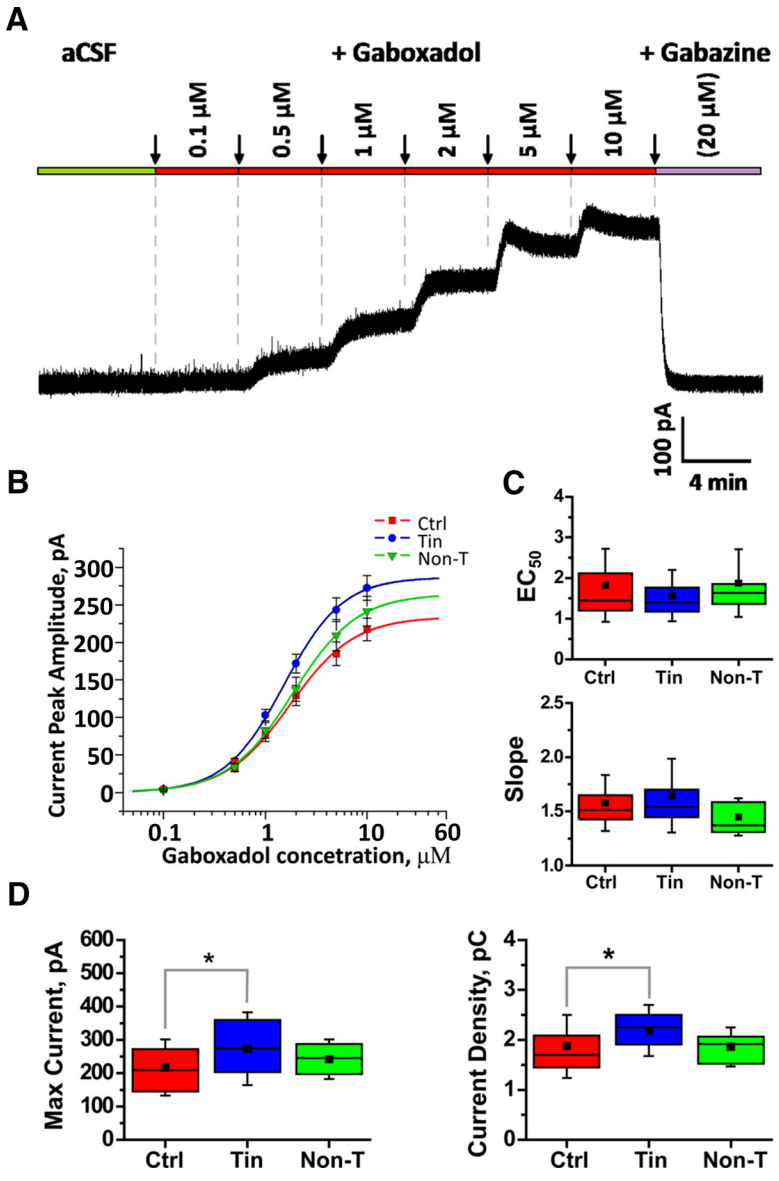

Figure 6. Extrasynaptic $GABA_A$R tonic inhibitory currents in MGB neurons increased in tinnitus rats. ***A***, Sample recording from an MGB neuron showing increasing tonic $GABA_A$ inhibitory current in response to bath application of increasing GBX doses (0.1–10 μM). The magnitude of this current is revealed by $GABA_A$R blockade with gabazine (40 μM). ***B***, Dose–response semi-log plot of tonic $GABA_A$ current mean amplitudes in control ($n = 32$ cells), sound-exposed nontinnitus ($n = 11$ cells), and sound-exposed tinnitus ($n = 43$ cells) groups of rats. Data were fitted with the logistic equation: $y = I_{min} + (I_{min} - I_{max})/(1 + (x/x_h)^p)$, where I_{min} and I_{max} are the minimal and maximal measured responses, respectively, x_h is the half-maximal effective concentration, and p is the absolute value of the slope of the curve. Tin rats showed significantly larger responses to increasing GBX doses. Data are presented as the mean ± SEM. ***C***, ***D***, For the highest dose tested, the maximal evoked current was significantly ($*p < 0.05$) different between control and tinnitus rats. Box charts for the highest dose show mean (square), median (middle line), 95% range (box limits), and SD (error bars). All recordings were performed contralaterally to noise exposure.

imize outward inhibitory Cl^- current in aCSF containing glutamate receptor antagonists (20 μM CNQX, 50 μM D-AP5). sIPSC ANOVA analysis revealed no significant group difference in phasic $GABA_A$ synaptic event frequency. Mean sIPSC frequencies were as follows: Ctrl, 4.64 ± 0.42 Hz ($n = 32$); Tin, 5.28 ± 0.41 Hz ($n = 43$); Non-T, 5.25 ± 0.67 Hz ($n = 11$). Furthermore, neither sIPSC amplitude (peak amplitude: Ctrl, 22.32 ± 1.54 pA, $n = 32$; Tin, 21.03 ± 0.59 pA, $n = 43$; Non-T: 18.64 ± 1.43 pA, $n = 11$) nor sIPSC duration (half-width: Ctrl, 12.70 ± 0.51 ms, $n = 32$; Tin, 12.29 ± 0.50 ms, $n = 43$; Non-T, 12.69 ± 0.71 ms, $n = 11$) demonstrated significant tinnitus-related changes. Cumulative probability plots and corresponding Kolmogorov–Smirnov statistical analysis further confirmed no significant differences in sIPSC properties, among any of the three groups (Fig. 8*B*). Adding 40 μM gabazine to the aCSF medium abolished sIPSCs in all recordings, confirming $GABA_A$R mediation of the sIPSCs.

Discussion

In the present study, we examined two hypotheses regarding GABAergic inhibitory function in the MGB that could underpin tinnitus produced by a peripheral acoustic insult. In MGB, either upregulation or downregulation of inhibitory function could underlie tinnitus-related thalamocortical hyperactivity and burst alterations in projections to AI, TRN, and amygdala (Kalappa et al., 2014).

Downregulation of inhibitory neurotransmission within the central auditory system is characteristic of partial peripheral deafferentation and is one feature associated with tinnitus-related pathology at multiple levels of the auditory neuraxis in different animal models (Caspary et al., 2008; Noreña, 2011; Gold and Bajo, 2014). Reduced inhibition is associated with abnormal neuronal hyperactivity, increased spontaneous firing rates, and, in some cases, bursting and synchronous oscillations. In DCN, tinnitus is associated with decreased inhibition, resulting in increased spontaneous and driven activity of projection neurons to IC (Brozoski et al., 2002; Wang et al., 2009; Roberts et al., 2010; Dehmel et al., 2012). Wang et al. (2009) found decreased neurochemical markers for glycinergic inhibition in DCN that was supported by patch-clamp studies showing decreased glycinergic function following sound exposure (Pilati et al., 2012b). In IC, markers for GABAergic neurotransmission were downregulated in models of tinnitus (Dong et al., 2010a,b; Gold and Bajo, 2014). Deafferentation and tinnitus models show increased spontaneous activity, peak spike rates within bursts, and rhythmicity of spiking in IC neurons (Bauer et al., 2008). Tinnitus-related downregulation of inhibition in the AI is thought to involve cortical receptive field reorganization, and cortical hyperactivity and bursting (Mühlnickel et al., 1998; Lanting et al., 2009; Yang et al., 2011; Brozoski et al., 2012).

Until recently, the role of GABAergic inhibition has not been thoroughly examined in MGB. MGB neurons function to filter and enhance incoming representation and perception of auditory features (Edeline, 2011; Bartlett, 2013). MGB engages high-level processing of auditory information through thalamocortical/corticothalamic interactions (Sherman, 2012). Winer et al. (2005) noted that descending cortical axons projecting to thalamus are more numerous than ascending projections (Jones,

1975; Ojima and Rouiller, 2010; Sherman, 2012). MGB has intricate connections with the limbic system that are likely involved in the emotional aspect of tinnitus (Sah et al., 2003; LeDoux, 2007; Kraus and Canlon, 2012). A potential role of MGB in tinnitus pathology has been outlined by Leaver et al. (2011) and Rauschecker et al. (2010), and the role of GABA in the pathology of chronic pain and tinnitus at the level of thalamus is integral to the thalamocortical dysrhythmia hypothesis (Llinás et al., 1999, 2005; Llinás and Steriade, 2006).

GABAergic inhibition plays a critical role in shaping MGB neuronal response properties (Cotillon-Williams et al., 2008; Cai et al., 2014; Mellott et al., 2014). Apart from synaptic $GABA_A$Rs that mediate fast signal transmission, MGB neurons show robust slow tonic inhibitory currents, mediated by $\alpha4\beta2\delta$-containing $GABA_A$Rs (Richardson et al., 2011, 2013; Yagüe et al., 2013). These high-affinity extrasynaptic $GABA_A$Rs appear to detect fluctuations in ambient GABA levels and may mediate ~90% of total inhibitory current in sensory thalamus (Belelli et al., 2005; Cope et al., 2005). Both hypotheses regarding GABAergic dysfunction in tinnitus-related pathology in MGB suggest altered GABAergic function related to deafferentation, but differ in the direction of tinnitus-related changes. DCN, IC, and AI circuits in tinnitus models show downregulation of inhibitory neurotransmission. Neurons in these structures show increased spontaneous activity, abnormal sound-evoked activity, spontaneous neuronal hyperactivity, and decreased neurochemical markers of GABA and/or glycine.

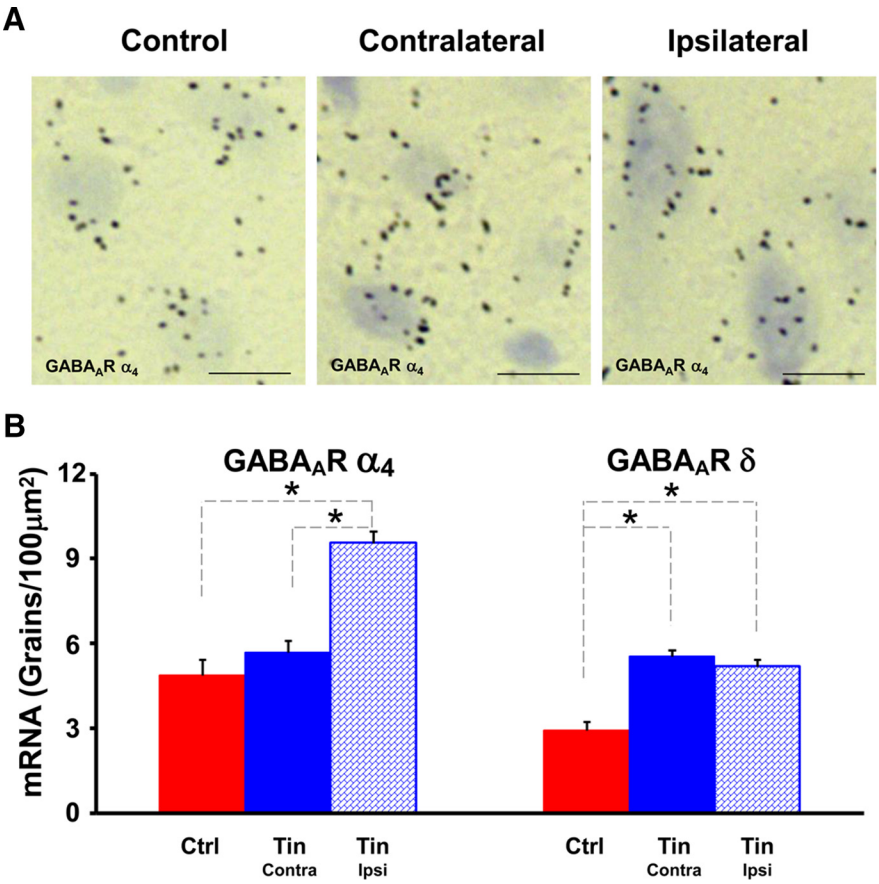

Figure 7. Tinnitus-related increase in MGB neuronal gene expression levels for α_4 and δ $GABA_A$R subunits. ***A***, Silver grains representing α_4 $GABA_A$R subunit mRNA are seen over neurons in the vMGB. Note the higher numbers of grains over neurons from sound-exposed animals. Scale bar, 10 μm. ***B***, Histogram shows α_4 and δ MGB neuron $GABA_A$R subunit mRNA changes (grain counts) from control ($n = 7$) and sound-exposed ($n = 6$) FBN rats. $GABA_A$R δ-subunit gene expression showed significant tinnitus-related increases both contralateral (Contra) and ipsilateral (Ipsi) to the sound exposure ($p < 0.001$). MGB changes in δ gene expression were observed both in dorsal and ventral MGB subdivisions. $GABA_A$Rs formed by δ-subunits are associated with extrasynaptic tonic inhibitory currents and extrasynaptic locations of $GABA_A$Rs. Interestingly, the α_4 mRNA level in MGB was significantly increased only ipsilateral to the sound exposure ($p < 0.001$).

Here we examined whether the loss or gain of GABAergic inhibition, underpinning thalamocortical dysrhythmia (Llinás et al., 1999, 2005; Llinás and Steriade, 2006), is the operative condition in MGB tinnitus pathology. The thalamocortical dysrhythmia hypothesis suggests that increased GABAergic inhibition leads to deinactivation of T-type Ca^{+2} channels for a subset of thalamocortical neurons, resulting in increased/abnormal bursting and increased MGB output (Kalappa et al., 2014). The present study found no evidence to support a downregulation of GABAergic inhibitory function in MGB. We show for the first time that 2 months following a tinnitus-inducing traumatic sound exposure, thalamocortical MGB neurons contralateral to sound exposure showed significantly increased duration of evoked bursting and increased gaboxadol-evoked tonic currents. The increase in maximum gaboxadol-evoked tonic current was evident in both the vMGB and dMGB, and suggests increased expression/density of functional extrasynaptic $GABA_A$Rs. This GBX-evoked increase in tonic current does not appear to be a simple consequence of the sound exposure since tonic $GABA_A$R currents recorded in Non-T animals were not significantly different from Ctrl group. Considering that tonic extrasynaptic GABAergic inhibition may account for ~80–90% of total inhibition in thalamus (Belelli et al., 2005; Cope et al., 2005), this moderate increase in $GABA_A$ tonic current in MGB neurons could significantly alter the response properties of thalamocortical neurons exposed to ambient GABA or GABA from synaptic spillover, altering auditory gating (Kalappa et al., 2014).

In support of our patch-clamp results, a significant tinnitus-related increase in $GABA_A$R δ-subunit mRNA level was found contralateral to the sound exposure. δ-Subunits are associated with extrasynaptic $GABA_A$Rs and tonic inhibition. The tinnitus-related upregulation of $GABA_A$R tonic inhibition markers are in stark contrast to a recent study (Richardson et al., 2013) that showed a near 50% age-related loss of functional and neurochemical markers of extrasynaptic $GABA_A$Rs in MGB.

It is also plausible that α_5-subunit-containing $GABA_A$Rs could contribute to tinnitus-related pathology by increasing tonic inhibition observed in MGB. We feel that a tinnitus-related upregulation is unlikely to account for the observed changes in the present study since α_5-subunit expression in thalamus is low compared with that in δ-containing $GABA_A$Rs (Sur et al., 1999; Pirker et al., 2000). It is especially low when expression levels in hippocampus and cortical layer 5 are compared (Pirker et al., 2000; Atack et al., 2005; Walker and Semyanov, 2008). In contrast, MGB has some of the highest expression levels of $\alpha_4\delta$-

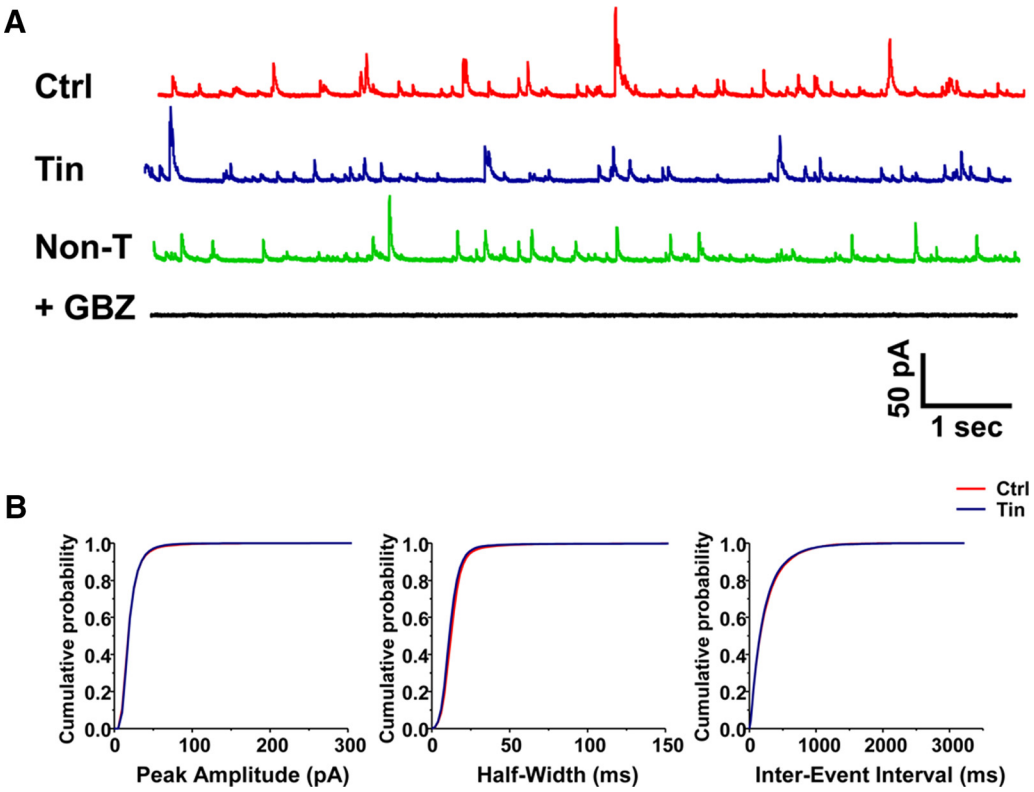

Figure 8. GABAergic synaptic inhibition is not altered in MGB neurons of tinnitus rats. ***A***, Representative traces of sIPSC recordings from MGB neurons from the Ctrl, Non-T, and Tin groups. Recordings were performed at +20 mV in the presence of 20 μM DNQX and 50 μM AP-5. Bath application of gabazine (GBZ) blocked all inhibitory $GABA_A$R-mediated synaptic events. ***B***, Averaged cumulative probability plots of sIPSC interevent intervals, amplitude, and half-width of MGB neurons in the Ctrl and Tin groups. Statistical analysis revealed no significant difference in these three GABAergic synaptic event parameters between the Ctrl and Tin groups (Ctrl, $n = 29$ cells; Tin, $n = 29$ cells). All recordings were contralateral to the sound exposure. Data are reported as the mean ± SEM.

receptors in the brain (Richardson et al., 2011; Wafford, 2014). Gaboxadol is a selective agonist for $\alpha_4\delta$-containing extrasynaptic $GABA_A$Rs at the concentrations used in the present study (Belelli et al., 2005). The extrasynaptic action of gaboxadol is supported by its lack of significant effect on spontaneous or miniature IPSCs in MGB neurons. Future studies will examine the role of α_5-containing constructs in the pathology of tinnitus.

The kinetics of gaboxadol-evoked extrasynaptic $GABA_A$R currents were not different among experimental groups, suggesting that $GABA_A$R extrasynaptic subunit composition may not be altered in animals with behavioral evidence of tinnitus.

Analysis of synaptic currents, sIPSCs, revealed no significant differences among groups. This suggests that synaptic MGB $GABA_A$ neurotransmission was not downregulated in tinnitus-related pathology. These data differ from findings with sodium salicylate-induced tinnitus that demonstrated reduced evoked synaptic transmission in MGB (Su et al., 2012).

In the present study, passive membrane properties of MGB neurons, including resting membrane potential, were not affected by tinnitus-related pathology. While extrasynaptic $GABA_A$Rs can be activated at low ambient concentrations of GABA, we were unable to consistently demonstrate an endogenous tonic current with $GABA_A$R blockade. The lack of significant gabazine effect on MGB neuron V_{rest} could be a function of aCSF flow rate in our slice preparation, resulting in low exogenous concentrations of ambient GABA. All recordings were made at room temperature, which could negatively impact ambient GABA levels (Iversen et al., 1968). A similar lack of endogenous $GABA_A$R tonic current was extensively examined for hypoglossal motor neurons (Numata et al., 2012). The present study did not test the possibility that changes in GABA uptake (GABA transporter, GAT1 or GAT3/4) could underpin tinnitus-related pathology in light of studies in models of absence epilepsy, where changes in GAT1 function have been described (Pirttimaki et al., 2013; Walker and Pavlov, 2014). Future studies will examine changes in GAT function.

The majority of MGB neurons responded to somatic depolarization with burst firing in Ctrl and Tin groups. However, neurons from Tin animals fired significantly more spikes per burst relative to control MGB neurons, suggesting a tinnitus-related increase in intrinsic membrane excitability, perhaps attributed to altered K^+, Na^+, or Ca^{2+} conductance. The tinnitus-related increase in the number of spikes per burst was more common in vMGB, which also showed a trend toward an increase in the number of bursting neurons. The present *in vitro* findings are consistent with the recent *in vivo* single-unit findings from awake animals showing tinnitus-related increases in burst properties of MGB neurons that directly correlated with an increase in tinnitus severity score (Kalappa et al., 2014). Animals used in the study by Kalappa et al. (2014) were similarly sound exposed and behaviorally tested.

Thalamic neurons can switch from tonic firing to bursting (Llinás and Jahnsen, 1982; Carbone and Lux, 1984; Jahnsen and Llinás, 1984). Bursting is elicited when thalamic neurons are hyperpolarized and is supported by the activation of low-voltage T-type calcium channels that, upon activation, generate LTSs. However, there was no evidence found to support the LTS difference between the Ctrl and Tin groups. An increase in GABAergic

inhibition might indirectly affect Ca^{2+} balance and, in turn, modulate potassium channels. Brief activation of GABAergic inhibitory synapses in hippocampus results in elevated neuronal excitability by modulating intracellular calcium level and reducing the sensitivity of calcium-activated potassium channels (Nelson et al., 2003). A tinnitus-related increase in tonic $GABA_A$ inhibition in MGB might similarly, but indirectly, increase MGB neuron intrinsic excitability. Future studies will examine the role of tinnitus-related changes of ion channel conductances underpinning increased burst parameters of MGB neurons.

While a large body of literature suggests that inhibition is reduced in tinnitus pathology, our results in MGB support the possibility that excessive tonic inhibition in MGB may be involved in thalamocortical dysrhythmia (Llinás et al., 2005; De Ridder et al., 2015). Recent data supporting the thalamocortical dysrhythmia hypothesis come from a human magnetoencephalography study (Adjamian et al., 2012) that found increased oscillation in tinnitus patients in the delta band. Thalamocortical bursting mode of operation in local circuitry during vigilance leads to increase in a low-frequency oscillation. This creates the phenomenon of an edge effect when low-frequency firing may lead to cortical disinhibition (Llinás et al., 2005).

Enhanced tonic inhibition in the MGB neurons is one of many factors possibly initiating thalamocortical dysrhythmia. The shift to abnormal periodic bursting activity is hypothesized to be related to partial deafferentation of specific sensory thalamic nuclei and possibly reduced excitation, which could result in thalamic neurons becoming hyperpolarized (Llinás et al., 2005). In turn, reduced ascending thalamic input could lead to a decrease in the excitatory drive/input to the TRN and reduced firing rates at the cortical level. Apart from the observed tinnitus-related increase in tonic inhibitory tone, other changes in thalamic neuronal membrane currents could mediate abnormal hyperpolarization associated with bursting activity. For example, resting membrane potential of thalamic neurons depends on the activity of two-pore-domain potassium (KCNK) channels, which are major targets for endogenous modulators (Talley et al., 2001; Musset et al., 2006). An increase in KCNK resting potassium current due to modulation and concomitant membrane hyperpolarization could effectively shift thalamic neurons into burst mode.

Another candidate for abnormal increased thalamocortical neurons bursting is hyperpolarization-activated cation (HCN) channels. HCN channels act as pacemaker channels where HCN current produces a depolarization of the membrane potential followed by LTS. Mice lacking HCN2 channels suffer from absence epilepsy, probably due to the increased responsiveness of thalamocortical neurons (Ludwig et al., 2003). Lack of HCN2 channels leads to hyperpolarization of thalamocortical neurons, promoting the recovery of T-type calcium channels from inactivation. This results in increased burst firing and oscillatory activity. Correspondingly, abnormal reduction in HCN current in thalamocortical neurons could be a mechanism generating thalamocortical dysrhythmia. Finally, an alteration in T-type calcium channel kinetics similarly modulates the bursting activity of thalamic neurons. It would be important to further explore other functional and molecular mechanisms at the MGB level involved in the thalamocortical dysrhythmia model and in tinnitus pathology.

In conclusion, the present study demonstrated that contrary to findings in other central auditory structures that have a tinnitus-related downregulation of functional and neurochemical markers of inhibitory neurotransmission, MGB circuits show no reduction of function. Rather, there was evidence of increased tonic $GABA_AR$ currents and an increased number of spikes per burst in animals with behavioral evidence of tinnitus. These results agree with, and partially support, the thalamocortical dysthymia model of tinnitus.

References

Adjamian P, Sereda M, Zobay O, Hall DA, Palmer AR (2012) Neuromagnetic indicators of tinnitus and tinnitus masking in patients with and without hearing loss. J Assoc Res Otolaryngol 13:715–731. CrossRef Medline

Atack JR, Alder L, Cook SM, Smith AJ, McKernan RM (2005) In vivo labelling of alpha5 subunit-containing GABA(A) receptors using the selective radioligand [(3)H]L-655,708. Neuropharmacology 49:220–229. CrossRef Medline

Banks MI, Smith PH (2011) Thalamocortical relations. In: The auditory cortex (Winer JA, Schreiner CE, eds), pp 75–98. New York: Springer.

Barberis A, Petrini EM, Mozrzymas JW (2011) Impact of synaptic neurotransmitter concentration time course on the kinetics and pharmacological modulation of inhibitory synaptic currents. Front Cell Neurosci 5:6. CrossRef Medline

Bartlett EL (2013) The organization and physiology of the auditory thalamus and its role in processing acoustic features important for speech perception. Brain Lang 126:29–48. CrossRef Medline

Bartlett EL, Smith PH (1999) Anatomic, intrinsic, and synaptic properties of dorsal and ventral division neurons in rat medial geniculate body. J Neurophysiol 81:1999–2016. Medline

Bauer CA, Brozoski TJ (2001) Assessing tinnitus and prospective tinnitus therapeutics using a psychophysical animal model. J Assoc Res Otolaryngol 2:54–64. CrossRef Medline

Bauer CA, Brozoski TJ, Rojas R, Boley J, Wyder M (1999) Behavioral model of chronic tinnitus in rats. Otolaryngol Head Neck Surg 121:457–462. CrossRef Medline

Bauer CA, Brozoski TJ, Myers K (2007) Primary afferent dendrite degeneration as a cause of tinnitus. J Neurosci Res 85:1489–1498. CrossRef Medline

Bauer CA, Turner JG, Caspary DM, Myers KS, Brozoski TJ (2008) Tinnitus and inferior colliculus activity in chinchillas related to three distinct patterns of cochlear trauma. J Neurosci Res 86:2564–2578. CrossRef Medline

Belelli D, Peden DR, Rosahl TW, Wafford KA, Lambert JJ (2005) Extrasynaptic $GABA_A$ receptors of thalamocortical neurons: a molecular target for hypnotics. J Neurosci 25:11513–11520. CrossRef Medline

Brickley SG, Mody I (2012) Extrasynaptic GABA(A) receptors: their function in the CNS and implications for disease. Neuron 73:23–34. CrossRef Medline

Brozoski TJ, Bauer CA, Caspary DM (2002) Elevated fusiform cell activity in the dorsal cochlear nucleus of chinchillas with psychophysical evidence of tinnitus. J Neurosci 22:2383–2390. Medline

Brozoski T, Odintsov B, Bauer C (2012) Gamma-aminobutyric acid and glutamic acid levels in the auditory pathway of rats with chronic tinnitus: a direct determination using high resolution point-resolved proton magnetic resonance spectroscopy (H-MRS). Front Syst Neurosci 6:9. CrossRef Medline

Cai R, Kalappa BI, Brozoski TJ, Ling LL, Caspary DM (2014) Is GABA neurotransmission enhanced in auditory thalamus relative to inferior colliculus? J Neurophysiol 111:229–238. CrossRef Medline

Carbone E, Lux HD (1984) A low voltage-activated, fully inactivating Ca channel in vertebrate sensory neurones. Nature 310:501–502. CrossRef Medline

Caspary DM, Ling L, Turner JG, Hughes LF (2008) Inhibitory neurotransmission, plasticity and aging in the mammalian central auditory system. J Exp Biol 211:1781–1791. CrossRef Medline

Cope DW, Hughes SW, Crunelli V (2005) $GABA_A$ receptor-mediated tonic inhibition in thalamic neurons. J Neurosci 25:11553–11563. CrossRef Medline

Cope DW, Di Giovanni G, Fyson SJ, Orbán G, Errington AC, Lorincz ML, Gould TM, Carter DA, Crunelli V (2009) Enhanced tonic GABAA inhibition in typical absence epilepsy. Nat Med 15:1392–1398. CrossRef Medline

Cotillon-Williams N, Huetz C, Hennevin E, Edeline JM (2008) Tonotopic control of auditory thalamus frequency tuning by reticular thalamic neurons. J Neurophysiol 99:1137–1151. CrossRef Medline

Dehmel S, Pradhan S, Koehler S, Bledsoe S, Shore S (2012) Noise overexpo-

sure alters long-term somatosensory-auditory processing in the dorsal cochlear nucleus—possible basis for tinnitus-related hyperactivity? J Neurosci 32:1660–1671. CrossRef Medline

De Ridder D, Vanneste S, Langguth B, Llinás R (2015) Thalamocortical dysrhythmia: a theoretical update in tinnitus. Front Neurol 6:124.

Dong S, Mulders WH, Rodger J, Robertson D (2009) Changes in neuronal activity and gene expression in guinea-pig auditory brainstem after unilateral partial hearing loss. Neuroscience 159:1164–1174. CrossRef Medline

Dong S, Rodger J, Mulders WH, Robertson D (2010a) Tonotopic changes in GABA receptor expression in guinea pig inferior colliculus after partial unilateral hearing loss. Brain Res 1342:24–32. CrossRef Medline

Dong S, Mulders WH, Rodger J, Woo S, Robertson D (2010b) Acoustic trauma evokes hyperactivity and changes in gene expression in guinea-pig auditory brainstem. Eur J Neurosci 31:1616–1628. CrossRef Medline

Edeline J-M (2011) Physiological properties of neurons in the medial geniculate body. In: The auditory cortex (Winer JA, Schreiner CE, eds), pp 251–274. New York: Springer.

Eggermont JJ, Roberts LE (2004) The neuroscience of tinnitus. Trends Neurosci 27:676–682. CrossRef Medline

Farrant M, Nusser Z (2005) Variations on an inhibitory theme: phasic and tonic activation of GABA(A) receptors. Nat Rev Neurosci 6:215–229. CrossRef Medline

Gold JR, Bajo VM (2014) Insult-induced adaptive plasticity of the auditory system. Front Neurosci 8:110. CrossRef Medline

Ito T, Oliver DL (2012) The basic circuit of the IC: tectothalamic neurons with different patterns of synaptic organization send different messages to the thalamus. Front Neural Circuits 6:48. CrossRef Medline

Iversen LL, Neal MJ (1968) The uptake of [3H]GABA by slices of rat cerebral cortex. J Neurochem 15:1141–1149. CrossRef Medline

Jahnsen H, Llinás R (1984) Voltage-dependent burst-to-tonic switching of thalamic cell activity: an in vitro study. Arch Ital Biol 122:73–82. Medline

Jones EG (1975) Some aspects of the organization of the thalamic reticular complex. J Comp Neurol 162:285–308. Medline

Kalappa BI, Brozoski TJ, Turner JG, Caspary DM (2014) Single-unit hyperactivity and bursting in the auditory thalamus of awake rats directly correlates with behavioral evidence of tinnitus. J Physiol 592:5065–5078. CrossRef Medline

Kraus KS, Canlon B (2012) Neuronal connectivity and interactions between the auditory and limbic systems. Effects of noise and tinnitus. Hear Res 288:34–46. CrossRef Medline

Kujawa SG, Liberman MC (2009) Adding insult to injury: cochlear nerve degeneration after "temporary" noise-induced hearing loss. J Neurosci 29:14077–14085. CrossRef Medline

Lanting CP, de Kleine E, van Dijk P (2009) Neural activity underlying tinnitus generation: results from PET and fMRI. Hear Res 255:1–13. CrossRef Medline

Leaver AM, Renier L, Chevillet MA, Morgan S, Kim HJ, Rauschecker JP (2011) Dysregulation of limbic and auditory networks in tinnitus. Neuron 69:33–43. CrossRef Medline

LeDoux J (2007) The amygdala. Curr Biol 17:R868–R874. CrossRef Medline

Ling LL, Hughes LF, Caspary DM (2005) Age-related loss of the GABA synthetic enzyme glutamic acid decarboxylase in rat primary auditory cortex. Neuroscience 132:1103–1113. CrossRef Medline

Llinás R, Jahnsen H (1982) Electrophysiology of mammalian thalamic neurones in vitro. Nature 297:406–408. CrossRef Medline

Llinás RR, Steriade M (2006) Bursting of thalamic neurons and states of vigilance. J Neurophysiol 95:3297–3308. CrossRef Medline

Llinás RR, Ribary U, Jeanmonod D, Kronberg E, Mitra PP (1999) Thalamocortical dysrhythmia: a neurological and neuropsychiatric syndrome characterized by magnetoencephalography. Proc Natl Acad Sci U S A 96:15222–15227. CrossRef Medline

Llinás R, Urbano FJ, Leznik E, Ramírez RR, van Marle HJ (2005) Rhythmic and dysrhythmic thalamocortical dynamics: GABA systems and the edge effect. Trends Neurosci 28:325–333. CrossRef Medline

Ludwig A, Budde T, Stieber J, Moosmang S, Wahl C, Holthoff K, Langebartels A, Wotjak C, Munsch T, Zong X, Feil S, Feil R, Lancel M, Chien KR, Konnerth A, Pape HC, Biel M, Hofmann F (2003) Absence epilepsy and sinus dysrhythmia in mice lacking the pacemaker channel HCN2. EMBO J 22:216–224. CrossRef Medline

Mellott JG, Foster NL, Nakamoto KT, Motts SD, Schofield BR (2014) Distribution of GABAergic cells in the inferior colliculus that project to the thalamus. Front Neuroanat 8:17. CrossRef Medline

Middleton JW, Kiritani T, Pedersen C, Turner JG, Shepherd GM, Tzounopoulos T (2011) Mice with behavioral evidence of tinnitus exhibit dorsal cochlear nucleus hyperactivity because of decreased GABAergic inhibition. Proc Natl Acad Sci U S A 108:7601–7606. CrossRef Medline

Montero VM, Scott GL (1983) Ultrastructural identification of satellite interneurons in the rat dorsal lateral geniculate nucleus. Arch Biol Med Exp (Santiago) 16:343–360. Medline

Mozrzymas JW (2004) Dynamism of GABA(A) receptor activation shapes the "personality" of inhibitory synapses. Neuropharmacology 47:945–960. CrossRef Medline

Mozrzymas JW (2010) Pharmacological studies reveal novel aspects of the versatility of GABAA receptors. J Physiol 588:1381–1382. CrossRef Medline

Mühlnickel W, Elbert T, Taub E, Flor H (1998) Reorganization of auditory cortex in tinnitus. Proc Natl Acad Sci U S A 95:10340–10343. CrossRef Medline

Musset B, Meuth SG, Liu GX, Derst C, Wegner S, Pape HC, Budde T, Preisig-Müller R, Daut J (2006) Effects of divalent cations and spermine on the K+ channel TASK-3 and on the outward current in thalamic neurons. J Physiol 572:639–657. CrossRef Medline

Nelson AB, Krispel CM, Sekirnjak C, du Lac S (2003) Long-lasting increases in intrinsic excitability triggered by inhibition. Neuron 40:609–620. CrossRef Medline

Noreña AJ (2011) An integrative model of tinnitus based on a central gain controlling neural sensitivity. Neurosci Biobehav Rev 35:1089–1109. CrossRef Medline

Noreña AJ, Eggermont JJ (2003) Changes in spontaneous neural activity immediately after an acoustic trauma: implications for neural correlates of tinnitus. Hear Res 183:137–153. CrossRef Medline

Numata JM, van Brederode JF, Berger AJ (2012) Lack of an endogenous GABAA receptor-mediated tonic current in hypoglossal motoneurons. J Physiol 590:2965–2976. CrossRef Medline

Ojima H, Rouiller EM (2010) Auditory cortical projections to the medial geniculate body. In: The auditory cortex (Winer JA, Schreiner CE, eds), pp 171–188. New York: Springer.

Peruzzi D, Bartlett E, Smith PH, Oliver DL (1997) A monosynaptic GABAergic input from the inferior colliculus to the medial geniculate body in rat. J Neurosci 17:3766–3777. Medline

Pilati N, Large C, Forsythe ID, Hamann M (2012a) Acoustic over-exposure triggers burst firing in dorsal cochlear nucleus fusiform cells. Hear Res 283:98–106. CrossRef Medline

Pilati N, Ison MJ, Barker M, Mulheran M, Large CH, Forsythe ID, Matthias J, Hamann M (2012b) Mechanisms contributing to central excitability changes during hearing loss. Proc Natl Acad Sci U S A 109:8292–8297. CrossRef Medline

Pirker S, Schwarzer C, Wieselthaler A, Sieghart W, Sperk G (2000) GABA(A) receptors: immunocytochemical distribution of 13 subunits in the adult rat brain. Neuroscience 101:815–850. CrossRef Medline

Pirttimaki T, Parri HR, Crunelli V (2013) Astrocytic GABA transporter GAT-1 dysfunction in experimental absence seizures. J Physiol 591:823–833. CrossRef Medline

Rauschecker JP, Leaver AM, Mühlau M (2010) Tuning out the noise: limbic-auditory interactions in tinnitus. Neuron 66:819–826. CrossRef Medline

Richardson BD, Ling LL, Uteshev VV, Caspary DM (2011) Extrasynaptic GABA(A) receptors and tonic inhibition in rat auditory thalamus. PLoS One 6:e16508. CrossRef Medline

Richardson BD, Brozoski TJ, Ling LL, Caspary DM (2012) Targeting inhibitory neurotransmission in tinnitus. Brain Res 1485:77–87. CrossRef Medline

Richardson BD, Ling LL, Uteshev VV, Caspary DM (2013) Reduced $GABA_A$ receptor-mediated tonic inhibition in aged rat auditory thalamus. J Neurosci 33:1218–1227a. CrossRef Medline

Roberts LE, Eggermont JJ, Caspary DM, Shore SE, Melcher JR, Kaltenbach JA (2010) Ringing ears: the neuroscience of tinnitus. J Neurosci 30:14972–14979. CrossRef Medline

Roberts LE, Bosnyak DJ, Thompson DC (2012) Neural plasticity expressed in central auditory structures with and without tinnitus. Front Syst Neurosci 6:40. CrossRef Medline

Rouiller EM, Colomb E, Capt M, De Ribaupierre F (1985) Projections of the reticular complex of the thalamus onto physiologically characterized regions of the medial geniculate body. Neurosci Lett 53:227–232. CrossRef Medline

Sah P, Faber ES, Lopez De Armentia M, Power J (2003) The amygdaloid complex: anatomy and physiology. Physiol Rev 83:803–834. CrossRef Medline

Sherman SM (2012) Thalamocortical interactions. Curr Opin Neurobiol 22:575–579. CrossRef Medline

Su YY, Luo B, Jin Y, Wu SH, Lobarinas E, Salvi RJ, Chen L (2012) Altered neuronal intrinsic properties and reduced synaptic transmission of the rat's medial geniculate body in salicylate-induced tinnitus. PLoS One 7:e46969. CrossRef Medline

Sur C, Farrar SJ, Kerby J, Whiting PJ, Atack JR, McKernan RM (1999) Preferential coassembly of alpha4 and delta subunits of the gamma-aminobutyric acidA receptor in rat thalamus. Mol Pharmacol 56:110–115. CrossRef Medline

Talley EM, Solorzano G, Lei Q, Kim D, Bayliss DA (2001) CNS distribution of members of the two-pore-domain (KCNK) potassium channel family. J Neurosci 21:7491–7505. Medline

Turner JG (2007) Behavioral measures of tinnitus in laboratory animals. Prog Brain Res 166:147–156. CrossRef Medline

Turner JG, Parrish J (2008) Gap detection methods for assessing salicylate-induced tinnitus and hyperacusis in rats. Am J Audiol 17:S185–192. CrossRef Medline

Turner JG, Brozoski TJ, Bauer CA, Parrish JL, Myers K, Hughes LF, Caspary DM (2006) Gap detection deficits in rats with tinnitus: a potential novel screening tool. Behav Neurosci 120:188–195. CrossRef Medline

Wafford KA (2014) The pharmacology of extrasynaptic GABAA receptors. In: Extrasynaptic GABAA receptors (Errington AC, Di Giovanni G, Crunelli V, eds), pp 51–74. New York: Springer.

Walker MC, Pavlov I (2014) The role of extrasynaptic GABAA receptors in focal epilepsy. In: Extrasynaptic GABAA receptors (Errington AC, Di Giovanni G, Crunelli V, eds), pp 207–221. New York: Springer.

Walker MC, Semyanov A (2008) Regulation of excitability by extrasynaptic GABA(A) receptors. Results Probl Cell Differ 44:29–48. CrossRef Medline

Walton KD, Llinás RR (2010) Central pain as a thalamocortical dysrhythmia: a thalamic efference disconnection? In: Translational pain research: from mouse to man, Chap 13 (Kruger L, Light AR, eds). Boca Raton, FL: CRC.

Wang H, Brozoski TJ, Turner JG, Ling L, Parrish JL, Hughes LF, Caspary DM (2009) Plasticity at glycinergic synapses in dorsal cochlear nucleus of rats with behavioral evidence of tinnitus. Neuroscience 164:747–759. CrossRef Medline

Wang X, Lu T, Bendor D, Bartlett E (2008) Neural coding of temporal information in auditory thalamus and cortex. Neuroscience 154:294–303. CrossRef Medline

Winer JA, Larue DT (1996) Evolution of GABAergic circuitry in the mammalian medial geniculate body. Proc Natl Acad Sci U S A 93:3083–3087. CrossRef Medline

Winer JA, Saint Marie RL, Larue DT, Oliver DL (1996) GABAergic feedforward projections from the inferior colliculus to the medial geniculate body. Proc Natl Acad Sci U S A 93:8005–8010. CrossRef Medline

Winer JA, Miller LM, Lee CC, Schreiner CE (2005) Auditory thalamocortical transformation: structure and function. Trends Neurosci 28:255–263. CrossRef Medline

Wisden W, Herb A, Wieland H, Keinanen K, Lüddens H, Seeburg PH (1991) Cloning, pharmacological characteristics and expression pattern of the rat GABAA receptor alpha 4 subunit. FEBS Lett 289:227–230. CrossRef Medline

Yagüe JG, Cavaccini A, Errington AC, Crunelli V, Di Giovanni G (2013) Dopaminergic modulation of tonic but not phasic GABAA-receptor-mediated current in the ventrobasal thalamus of Wistar and GAERS rats. Exp Neurol 247:1–7. CrossRef Medline

Yang G, Lobarinas E, Zhang L, Turner J, Stolzberg D, Salvi R, Sun W (2007) Salicylate induced tinnitus: behavioral measures and neural activity in auditory cortex of awake rats. Hear Res 226:244–253. CrossRef Medline

Yang S, Weiner BD, Zhang LS, Cho SJ, Bao S (2011) Homeostatic plasticity drives tinnitus perception in an animal model. Proc Natl Acad Sci U S A 108:14974–14979. CrossRef Medline